

Mode III SIFs for interface cracks in an FGM coating-substrate system

Mojtaba Mahmoudi Monfared*

Department of Mechanical Engineering, Hashtgerd Branch, Islamic Azad University, P.O. Box 33615-178, Alborz, Iran

(Received May 26, 2017, Revised July 7, 2017, Accepted July 11, 2017)

Abstract. In this study, interaction of several interface cracks located between a functionally graded material (FGM) layer and an elastic layer under anti-plane deformation based on the distributed dislocation technique (DDT) is analyzed. The variation of the shear modulus of the functionally graded coating is modeled by an exponential and linear function along the thickness of the layer. The complex Fourier transform is applied to governing equation to derive a system of singular integral equations with Cauchy type kernel. These equations are solved by a numerical method to obtain the stress intensity factors (SIFs) at the crack tips. The effects of non-homogeneity parameters for exponentially and linearly form of shear modulus, the thickness of the layers and the length of crack on the SIFs for several interface cracks are investigated. The results reveal that the magnitude of SIFs decrease with increasing of FG parameter and thickness of FGM layer. The values of SIFs for FGM layer with exponential form is less than the linear form.

Keywords: FGM coating; distributed dislocation technique; multiple interface cracks; stress intensity factors; singular integrals equations

1. Introduction

Since use of functionally graded materials (FGMs) has been increased in engineering applications such as a thermal coating barrier, a preventer from chemical corrosion or oxidation etc. The fracture analysis is important for FGMs and has absorbed the attention of many researchers in recent years. The analytical expression for stress intensity factor (SIFs) in two bonded elastic layers containing cracks perpendicular to and on the interface was studied by Ming-Che and Erdogan (1983). The problem was formulated in the terms of integral equations and the singular behavior of the solution near and at the ends of intersection of the cracks. The numerical method of part I for solving problem of plane, containing crack with various crack geometry perpendicular to and on the interface of the two layers was analyzed by Ming-Che and Erdogan (1983). The singular nature of the crack tip stress field in a non-homogeneous medium having a shear modulus with a discontinuous derivative was investigated by Erdogan (1985). He has shown that the square root singularity of the crack tip stress field is unaffected by the discontinuity in the derivative of the shear modulus. The problem of an interface crack between two bonded homogeneous and non-homogeneous half planes was solved by Delale and Erdogan (1988). The asymptotic stress and displacement fields of a propagating interface crack under mode III conditions by use of eigenfunction expansion technique was provided by Chiang (1989). The stress singularity at crack tips located at the interface between two different power-law materials under mode III loading was discussed by Champion and Atkinson

(1990). Various aspects of stress fields near an interface crack in three-dimensional bi-material plates were investigated by Nakamura (1991). Erdogan *et al.* (1991) solved the mode III crack problem for two bonded homogeneous half planes. The interfacial zone was modeled by a non-homogeneous strip in such a way that the shear modulus is a continuous function throughout the composite medium and has discontinuous derivatives along the boundaries of the interfacial zone. It was shown that the stresses had the standard square root singularity. Erdogan and Wu (1993) studied the influence of the structure and thickness of the interfacial regions on the strain energy release rate in bonded isotropic or orthotropic materials containing collinear interface cracks. They have formulated the problem in terms of a system of singular integral equations of second kind which is solved by using a relatively simple and efficient technique. The results showed that the effect of properties and the relative thickness of the interfacial region on the stress intensity factors and the strain energy release rate can be highly significant. Jin and Batra (1995) have investigated the interface cracking between ceramic and/or functionally graded coatings and a substrate under anti-plane shear. In this work, various coating models such as single layered homogeneous coating, double layered piece-wise homogeneous coating, single layered FGM coating and double layered coating with an FGM bottom coat were analyzed. Chan *et al.* (2001) have solved a displacement based integral equation formulation for the mode III crack problem in a non-homogeneous medium with a continuously differentiable shear modulus, which is assumed to be an exponential function. Lu *et al.* (2001) obtained the analytical solution for mode III interface crack which propagates along the interface of two joined media. The interface crack problem in graded orthotropic media

*Corresponding author, Assistant Professor
E-mail: mo_m_monfared@yahoo.com

was analyzed by Dag *et al.* (2004). Mechanical properties of the medium were assumed to be continuous with discontinuous derivatives at the interface. Crack tips stress fields for a crack along the direction of property gradation in functionally graded materials obtained by Jain *et al.* (2004). In this study, material property was assumed linearly along the gradation direction. The plane elasticity problem for a functionally graded strip under in-plane loading considered by Zhanqi and Zheng (2006). In their work, the influences of the geometric parameters and the graded parameter on the stress intensity factors and on the strain energy release rate were investigated. Lu *et al.* (2007) have investigated the asymmetrical dynamic propagation problems of mode III interface crack under the condition of point loads and unit-step loads by the application of the theory of complex functions. Mode III crack problem in a bi-FGM composite was examined by Li *et al.* (2008). Chen and Chue (2009) have dealt with the anti-plane problems of two bonded FGM strips weakened by an internal crack normal to the interface. The material properties are assumed to vary exponentially along of the direction of the crack lines. The derived system of singular integral equations was solved numerically by Gauss-Chebyshev integration formula. Yang *et al.* (2009) studied the fracture problems near the interface crack tip of double dissimilar orthotropic composite materials. With the help of complex function method, the singularity exponents are derived and determined. Chue and Yeh (2010) considered the anti-plane crack problem of two bonded FGM strips. Each strip concludes an arbitrarily oriented crack and the material properties are assumed in exponential forms. Kargarnovin *et al.* (2011) studied the anti-plane fracture mechanics in an FGM strip with an embedded crack. They have assumed that shear modulus varies in a linear form along the strip thickness. Asadi *et al.* (2012) have obtained the stress fields for an orthotropic strip with defects and imperfect FGM coating by using of the Volterra screw dislocation. The elastic shear modulus of coating was considered to vary exponentially. The dislocation solution is utilized to formulate integral equations for analyzing of multiple smooth cracks under anti-plane deformation. Cheng *et al.* (2012) studied the plane elasticity problem of two bonded dissimilar functionally graded strips containing of an interface crack in which material properties vary arbitrarily. The governing equations in terms of Airy stress function were formulated and the exact solutions of them were obtained for several special variations of material properties in the Fourier transformation domain. An interfacial penny-shaped crack between piezoelectric layer and elastic half-space investigated by Ren *et al.* (2014). Monfared and Ayatollahi (2015) calculated dynamic stress intensity factors of a cracked orthotropic half-plane bounded to functionally graded coating under anti-plane condition. In their work, the stress fields were obtained with Cauchy singularity at the location of dislocation and also the distributed dislocation technique was utilized to derive integral equations for multiple interacting cracks in an orthotropic half-plane with functionally graded orthotropic coating. Torshizian (2015) studied stress intensity factors in two-dimensional functionally graded materials under anti-

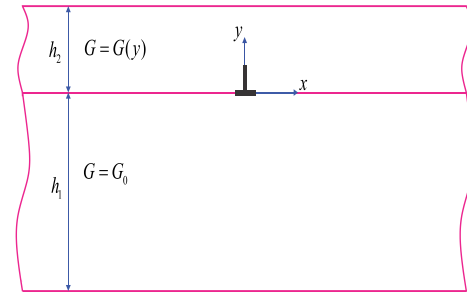


Fig. 1 Schematic view of the single dislocation at interface

plane deformation. The material properties were assumed to vary linearly along of the two planar directions and the problem was solved by using of the separating variables and Hankel transforms. Farahpour *et al.* (2015) investigated the stress intensity factor of a longitudinal semi-elliptical crack on the wall of an aluminum cylinder with FGM coating by using of the finite element method. They had studied the effect of functionally graded material coatings on the fracture behavior of semi-elliptical cracks in cylinders.

In this article, a functionally graded material bonded to an elastic substrate weakened by several interface cracks under anti-plane deformation by means of DDT is studied. Distributed dislocation technique is a powerful semi-analytical method for calculating accurate solutions to plane crack problems based on the principle of superposition (see Hills *et al.* 1996). In fact, the technique is excellent for solutions of complex crack patterns and any number of cracks (see Monfared and Bagheri 2016) and makes it an ideal tool for exploring problems involving inclusions, interfaces, pores, and similar features. The formulation for the any number and size of interface cracks has been explained in section 3.

It is assumed that the shear modulus of FGM coating varies along of the thickness of the layer exponentially and linearly function. The stress fields subjected to single Volterra screw dislocation has been located between two dissimilar materials is carried out. The distributed dislocation technique is utilized to perform a set of integral equations for dissimilar medium containing several interface cracks. The integral equations with Cauchy type singularities are solved numerically and SIFs are determined. The numerical examples are given to show the effects thickness of the FGM layer, the material properties and the length of the crack upon the fracture behavior.

2. Statement of problem

A homogeneous substrate with thickness h_1 bonded to a functionally graded coating with thickness h_2 containing a single Volterra type screw dislocation located at $y=0$ between the coating and substrate is described in Fig. 1. Two cases of material property models for the FGM coating are considered in the present study. The first case is an FGM coating with the shear modulus assumed to varies exponentially function along the thickness of layer and the second case is an FGM coating with linear function for shear modulus. Let the components of the displacement in

the x , y and z directions be labeled by u , v and w , respectively. For anti-plane deformation u and v vanish everywhere and w is the function of x , y . The constitutive relations between the displacement and stresses for FGM and homogeneous material may be expressed as follows

$$\begin{aligned} \tau_{zx} &= G(y) \frac{\partial w}{\partial x}, \quad \tau_{zy} = G(y) \frac{\partial w}{\partial y}, \quad 0 \leq y \leq h_2, \\ \tau_{zx} &= G_0 \frac{\partial w}{\partial x}, \quad \tau_{zy} = G_0 \frac{\partial w}{\partial y}, \quad -h_1 \leq y \leq 0, \end{aligned} \quad (1)$$

where $G(y)$ and G_0 are the shear modulus in the FG and homogeneous materials respectively. Substituting Eq. (1) into the equilibrium equation $\tau_{ij,j}=0$ can be written as

$$\begin{aligned} \frac{\partial^2 w}{\partial y^2} + \frac{\partial^2 w}{\partial x^2} + \frac{G'(y)}{G(y)} \frac{\partial w}{\partial y} &= 0, \quad 0 \leq y \leq h_2, \\ \frac{\partial^2 w}{\partial y^2} + \frac{\partial^2 w}{\partial x^2} &= 0, \quad -h_1 \leq y \leq 0. \end{aligned} \quad (2)$$

where $G'(y)$ is the derivative of $G(y)$. According to Fig. 1 the boundary and continuity conditions can be described as

$$\begin{aligned} \tau_{zy}(x, h_2) &= 0, \quad |x| < \infty, \\ \tau_{zy}(x, -h_1) &= 0, \quad |x| < \infty, \\ \tau_{zy}(x, 0^+) &= \tau_{zy}(x, 0^-), \\ w(x, 0^+) - w(x, 0^-) &= b_z H(x) \end{aligned} \quad (3)$$

where positive and negative signs used to represent the FGM and homogeneous layer respectively, b_z is Burgers vector which is located at origin and $H(\cdot)$ is the Heaviside-step function.

2.1 The first case, exponentially-varying properties

There are two material properties involved in this study. The shear modulus in the Eq. (1) for FG layer can be described exponential form of the type

$$\mu(y) = G_0 e^{\beta y} \quad (4)$$

where β is a non-homogeneity parameter with the dimension of $(\text{length})^{-1}$. With substituting Eq. (4) into Eq. (2), we obtain

$$\begin{aligned} \frac{\partial^2 w}{\partial y^2} + \frac{\partial^2 w}{\partial x^2} + \beta \frac{\partial w}{\partial y} &= 0, \quad 0 \leq y \leq h_2, \\ \frac{\partial^2 w}{\partial y^2} + \frac{\partial^2 w}{\partial x^2} &= 0, \quad -h_1 \leq y \leq 0. \end{aligned} \quad (5)$$

Eq. (5) is solved by means of the complex Fourier transform which is defined by

$$F(\omega) = \int_{-\infty}^{\infty} f(x) e^{i\omega x} dx. \quad (6)$$

The inversion of Eq. (6) is

$$f(x) = \frac{1}{2\pi} \int_{-\infty}^{\infty} F(\omega) e^{-i\omega x} d\omega. \quad (7)$$

Application of Eq. (6) to Eq. (5) it can be shown that

$$\begin{aligned} w^*(\omega, y) &= A_1(\omega) e^{\lambda_1 y} + A_2(\omega) e^{\lambda_2 y}, \quad 0 \leq y \leq h_2, \\ w^*(\omega, y) &= B_1(\omega) e^{|\omega| y} + B_2(\omega) e^{-|\omega| y}, \quad -h_1 \leq y \leq 0. \end{aligned} \quad (8)$$

where w^* is the Fourier transform of displacement component, $A_1(\omega)$, $A_2(\omega)$, $B_1(\omega)$ and $B_2(\omega)$ are unknown functions of ω , and

$$\begin{aligned} \lambda_1(\omega) &= \frac{1}{2}[-\beta + \sqrt{\beta^2 + 4\omega^2}], \\ \lambda_2(\omega) &= \frac{1}{2}[-\beta - \sqrt{\beta^2 + 4\omega^2}]. \end{aligned} \quad (9)$$

Applying the Fourier transform to the Eq. (3) yields

$$\begin{aligned} \frac{dw^*(\omega, h_2)}{dy} &= 0, \quad \frac{dw^*(\omega, -h_1)}{dy} = 0, \\ \frac{dw^*(\omega, 0^+)}{dy} &= \frac{dw^*(\omega, 0^-)}{dy}, \\ w^*(\omega, 0^+) - w^*(\omega, 0^-) &= b_z (\pi \delta(\omega) + i/\omega). \end{aligned} \quad (10)$$

where $\delta(\cdot)$ is the Dirac delta function. By using conditions (10) the four unknown coefficients in Eq. (8) may be obtained as

$$\begin{aligned} A_2(\omega) &= -\frac{\lambda_1}{\lambda_2} e^{(\lambda_1 - \lambda_2)h_2} A_1(\omega), \quad B_2(\omega) = e^{-2|\omega|h_1} B_1(\omega), \\ A_1(\omega)\lambda_1 + A_2(\omega)\lambda_2 &= (B_1(\omega) - B_2(\omega))|\omega|, \\ B_1(\omega) &= b_z (\pi \delta(\omega) + i/\omega) P(\omega). \end{aligned} \quad (11)$$

in which

$$\begin{aligned} P(\omega) &= \lambda_1 \lambda_2 (e^{h_2(\lambda_1 - \lambda_2)} - 1) \\ &= \{ \lambda_1 [|\omega| - \lambda_2 - (|\omega| + \lambda_2) e^{-2|\omega|h_1}] e^{h_2(\lambda_1 - \lambda_2)} \\ &\quad + \lambda_2 [\lambda_1 - |\omega| + (|\omega| + \lambda_1) e^{-2|\omega|h_1}] \}. \end{aligned} \quad (12)$$

Substituting $B_1(\omega)$ and $B_2(\omega)$ in Eq. (11) into the Eq. (8) and in view of Eq.(7) the displacement field in elastic layer may be obtained as

$$\begin{aligned} w(x, y) &= -\frac{b_z (1 - e^{\beta h_2})}{2(1 - \beta h_1 - e^{\beta h_2})} \\ &\quad + \frac{ib_z}{2\pi} \int_{-\infty}^{\infty} \frac{P(\omega)}{\omega} [e^{|\omega| y} + e^{-|\omega|(y+2h_1)}] e^{-i\omega x} d\omega, \\ &\quad -h_1 \leq y \leq 0. \end{aligned} \quad (13)$$

It is convenient to integrals in Eq. (13) split into odd and even parts can be obtained as

$$\begin{aligned} w(x, y) &= -\frac{b_z (1 - e^{\beta h_2})}{2(1 - \beta h_1 - e^{\beta h_2})} \\ &\quad + \frac{b_z}{\pi} \int_0^{\infty} \frac{P(\omega)}{\omega} [e^{\omega y} + e^{-\omega(y+2h_1)}] \sin(\omega x) d\omega, \\ &\quad -h_1 \leq y \leq 0. \end{aligned} \quad (14)$$

The stress components in the elastic layer in view of Eqs. (1) and (14) obtained as

$$\begin{aligned}\tau_{zx}(x, y) &= \frac{b_z G_0}{\pi} \int_0^{\infty} P(\omega) [e^{\omega y} + e^{-\omega(y+2h_1)}] \cos(\omega x) d\omega, \\ \tau_{zy}(x, y) &= \frac{b_z G_0}{\pi} \int_0^{\infty} P(\omega) [e^{\omega y} - e^{-\omega(y+2h_1)}] \sin(\omega x) d\omega, \\ &-h_1 \leq y \leq 0.\end{aligned}\quad (15)$$

The integrals in Eq.(15) have a singularity behavior when parameter ω goes to the infinity, however, the singular part of integrals should be separated from the regular part. We determine the leading terms of Eq. (15) as, $\omega \rightarrow \infty$ employ the following identities

$$\begin{aligned}\int_0^{\infty} e^{-\omega y} \sin(\omega x) d\omega &= \frac{x}{x^2 + y^2}, \quad y > 0, \\ \int_0^{\infty} e^{-\omega y} \cos(\omega x) ds &= \frac{y}{x^2 + y^2}, \quad y > 0.\end{aligned}\quad (16)$$

The stress components in the elastic layer reduce to

$$\begin{aligned}\tau_{zx}(x, y) &= \frac{b_z G_0}{2\pi} \left\{ \frac{y}{x^2 + y^2} \right. \\ &+ \left. \int_0^{\infty} [2P(\omega) (e^{\omega y} + e^{-\omega(y+2h_1)}) + e^{\omega y}] \cos(\omega x) d\omega \right\}, \\ \tau_{zy}(x, y) &= \frac{b_z G_0}{2\pi} \left\{ -\frac{x}{x^2 + y^2} \right. \\ &+ \left. \int_0^{\infty} [2P(\omega) (e^{\omega y} - e^{-\omega(y+2h_1)}) + e^{\omega y}] \sin(\omega x) d\omega \right\}, \\ &-h_1 \leq y \leq 0.\end{aligned}\quad (17)$$

All of the integrals in Eq. (17) are regular and can be computed with numerical solutions.

2.2 The second case, linearly-varying properties

The second model is called linearly which shear modulus in Eq. (1) varies linearly in the thickness of the FGM layer is defined as follows

$$G(y) = G_0(1 + \beta y) \quad (18)$$

Substituting Eq. (18) into Eq. (2) we obtain

$$\begin{aligned}\frac{\partial^2 w}{\partial y^2} + \frac{\partial^2 w}{\partial x^2} + \frac{\beta}{1 + \beta y} \frac{\partial w}{\partial y} &= 0, \quad 0 \leq y \leq h_2, \\ \frac{\partial^2 w}{\partial y^2} + \frac{\partial^2 w}{\partial x^2} &= 0, \quad -h_1 \leq y \leq 0.\end{aligned}\quad (19)$$

By using Fourier transforms (6), solution of Eq. (19) may be obtained as follows:

$$\begin{aligned}w^*(\omega, y) &= C_1(\omega) I_0(\omega(1 + \beta y)/\beta) \\ &+ C_2(\omega) K_0(\omega(1 + \beta y)/\beta), \quad 0 \leq y \leq h_2\end{aligned}\quad (20)$$

$$w^*(\omega, y) = D_1(\omega) e^{|\omega|y} + D_2(\omega) e^{-|\omega|y}, \quad -h_1 \leq y \leq 0.$$

where $I_0(\cdot)$ and $K_0(\cdot)$ are the first and second kinds of zero

order modified Bessel functions, respectively. By using conditions (10) the four unknown coefficients in Eq. (20) may be obtained as

$$\begin{aligned}C_2(\omega) &= \frac{I_1(\omega(1 + \beta h_2)/\beta)}{K_1(\omega(1 + \beta h_2)/\beta)} C_1(\omega), \\ D_2(\omega) &= e^{-2|\omega|h_1} D_1(\omega), \\ \omega(C_1(\omega) I_1(\omega/\beta) - C_2(\omega) K_1(\omega/\beta)) &= |\omega|(D_1(\omega) - D_2(\omega)), \\ D_1(\omega) &= \frac{b_z Q(\omega) (\pi \delta(\omega) + i/\omega)}{R(\omega)}.\end{aligned}\quad (21)$$

in which

$$\begin{aligned}Q(\omega) &= -[I_1(\omega(1 + \beta h_2)/\beta) K_1(\omega/\beta) \\ &- I_1(\omega/\beta) K_1(\omega(1 + \beta h_2)/\beta)], \\ R(\omega) &= (1 + e^{-2|\omega|h_1}) [I_1(\omega(1 + \beta h_2)/\beta) K_1(\omega/\beta) \\ &- I_1(\omega/\beta) K_1(\omega(1 + \beta h_2)/\beta)] \\ &+ \text{sgn}(\omega) (1 - e^{-2|\omega|h_1}) [I_1(\omega(1 + \beta h_2)/\beta) K_0(\omega/\beta) \\ &+ I_0(\omega/\beta) K_1(\omega(1 + \beta h_2)/\beta)].\end{aligned}\quad (22)$$

In above Eq. (22) $\text{sgn}(\cdot)$ is the sign function, $I_1(\cdot)$ and $K_1(\cdot)$ are the first and second kinds of first order modified Bessel functions, respectively. Substituting $D_1(\omega)$ and $D_2(\omega)$ in Eq. (21) into the Eq. (20) and in view of Eq. (7) the displacement fields in elastic layer may be obtained as

$$\begin{aligned}w(x, y) &= -\frac{b_z h_2 (2 + \beta h_2)}{4h_1 + 2h_2 (2 + \beta h_2)} \\ &+ \frac{ib_z}{2\pi} \int_{-\infty}^{\infty} \frac{Q(\omega)}{\omega R(\omega)} \left(e^{|\omega|y} + e^{-|\omega|(y+2h_1)} \right) e^{-i\omega x} d\omega, \\ &-h_1 \leq y \leq 0.\end{aligned}\quad (23)$$

By changing the integral in Eq. (23) to the odd and even parts obtained as

$$\begin{aligned}w(x, y) &= -\frac{b_z h_2 (2 + \beta h_2)}{4h_1 + 2h_2 (2 + \beta h_2)} \\ &+ \frac{b_z}{\pi} \int_0^{\infty} \frac{Q(\omega)}{\omega R(\omega)} \left(e^{\omega y} + e^{-\omega(y+2h_1)} \right) \sin(\omega x) d\omega, \\ &-h_1 \leq y \leq 0.\end{aligned}\quad (24)$$

The stress components in the elastic layer in view of Eqs. (1) and (24) can be obtained as

$$\begin{aligned}\tau_{zx}(x, y) &= \frac{b_z G_0}{\pi} \int_0^{\infty} \frac{Q(\omega)}{R(\omega)} \left(e^{\omega y} + e^{-\omega(y+2h_1)} \right) \cos(\omega x) d\omega, \\ \tau_{zy}(x, y) &= \frac{b_z G_0}{\pi} \int_0^{\infty} \frac{Q(\omega)}{R(\omega)} \left(e^{\omega y} - e^{-\omega(y+2h_1)} \right) \sin(\omega x) d\omega, \\ &-h_1 \leq y \leq 0.\end{aligned}\quad (25)$$

The integrals in Eq. (25) do not converge for the points in the proximity of dislocation. Therefore, The asymptotic analysis of the integrands when $\omega \rightarrow \infty$ are needed. The first and second kinds of modified Bessel functions have the

following behaviours when argument ω tends to infinity

$$\begin{aligned}\lim_{|\omega| \rightarrow \infty} I_0(\omega) &= \lim_{|\omega| \rightarrow \infty} I_1(\omega) = \frac{e^{\omega}}{\sqrt{2\pi\omega}}, \\ \lim_{|\omega| \rightarrow \infty} K_0(\omega) &= \lim_{|\omega| \rightarrow \infty} K_1(\omega) = e^{-\omega} \sqrt{\frac{\pi}{2\omega}}.\end{aligned}\quad (26)$$

The stress components in the elastic layer in view of Eq. (16) reduce to

$$\begin{aligned}\tau_{zx}(x, y) &= \frac{b_z G_0}{2\pi} \left\{ \frac{y}{x^2 + y^2} \right. \\ &\quad \left. + \int_0^{\infty} \left[\frac{2Q(\omega)}{R(\omega)} \left(e^{\omega y} + e^{-\omega(y+2h_1)} \right) + e^{\omega y} \right] \cos(\omega x) d\omega \right\}, \\ \tau_{zy}(x, y) &= \frac{b_z G_0}{2\pi} \left\{ -\frac{x}{x^2 + y^2} \right. \\ &\quad \left. + \int_0^{\infty} \left[\frac{2Q(\omega)}{R(\omega)} \left(e^{\omega y} - e^{-\omega(y+2h_1)} \right) + e^{\omega y} \right] \sin(\omega x) d\omega \right\}, \\ &\quad -h_1 \leq y \leq 0.\end{aligned}\quad (27)$$

All of the integrals in Eq. (27) are regular and can be computed with numerical solutions.

3. Formulation of several interface cracks

The dislocation solutions accomplished in the preceding section may be employed to analyze several interface cracks. The stress components created by a single screw dislocation which is located at interface between two dissimilar layers can be written as

$$\tau_{zy}(x, y) = b_z \left\{ k_{zy}^q(x, y) \right\}, \quad -h_1 \leq y \leq 0, \quad (28)$$

where $k_{zy}^q(x, y)$, $q=1,2$ are the coefficients of b_z in Eqs. (17) and (27). Consider an elastic layer bonded to an FGM layer containing N interface cracks, configuration of cracks respect to the Cartesian coordinate x - y can be modeled in parametric forms as follows:

$$\begin{aligned}x_i(s) &= x_{i0} + c_i s, \\ y_i(s) &= y_{i0}, \quad i = 1, 2, \dots, N, \quad -1 \leq s \leq 1.\end{aligned}\quad (29)$$

where (x_{i0}, y_{i0}) is the center of coordinates and c_i is half length of the i -th crack, respectively. Suppose a crack which is created by a continuous distribution of generalized dislocations with unknown density $B_{zi}(t)$ are distributed on $c_i dt$ at the surface of the i -th crack. The anti-plane traction on the surface of i -th crack, due to the above distribution of dislocations on all N cracks are obtained. The system of singular integral equations can be written in the following form which will be utilized in numerical procedure.

$$-\tau_{zy}(x_i(s), y_i(s)) + \sum_{j=1}^N \int_{-1}^1 k_{ij}(s, p) c_j B_{zj}(t) dt = 0, \quad (30)$$

$$i = 1, 2, \dots, N.$$

Employing the definition of generalized dislocation

density function, the equation for the crack opening field displacement across the i -th crack yields

$$w_i^-(s) - w_i^+(s) = \int_{-1}^s c_j B_{zj}(t) dt, \quad i = 1, 2, \dots, N. \quad (31)$$

For an interfacial crack between two bonded dissimilar materials, Eq. (30) should be complimented with the following well-known closure requirements

$$\int_{-1}^1 B_{zi}(t) dt = 0, \quad i = 1, 2, \dots, N. \quad (32)$$

To compute the dislocation densities on the crack surfaces the system of Cauchy singular integral Eqs. (30) and (32) must be solved simultaneously. For this purpose, the Gauss-Chebyshev quadrature scheme for numerical estimation developed by Erdogan *et al.* (1973). Under anti-plane deformation stress field in the near of crack tips is square root singular at tip of interfacial cracks. Therefore, dislocation density, on the surface of cracks, is taken as

$$B_{zi}(t) = \frac{H_{zi}(t)}{\sqrt{1-t^2}}, \quad -1 < t < 1, \quad i = 1, 2, \dots, N. \quad (33)$$

$H_{zi}(t)$ obtain from substituting Eq. (33) into Eqs. (30) and (32) by using of the numerical technique of integral equations. The anti-plane stress intensity factors, based on the dislocation density functions are derived by Asadi *et al.* (2012) for elastic layer as follows

$$\begin{aligned}(k_{III})_{Li} &= \frac{G_0 \sqrt{c_i} H_{zi}(-1)}{2}, \\ (k_{III})_{Ri} &= -\frac{G_0 \sqrt{c_i} H_{zi}(1)}{2}, \quad i = 1, \dots, N.\end{aligned}\quad (34)$$

where the subscripts L and R designate the left and right crack tips, respectively.

4. Numerical example and discussion

The main results of this study are the calculation of the stress intensity factors for different non-homogeneity parameter, the crack length and interactions between several cracks which are located at interface. The validation of the formulation is accomplished by comparing our results with those obtained by Ding and Li (2008). It may be observed from Table 1 that the results obtained via DDT are in good agreement with those of Ding and Li (2008). The above presented method allows the consideration of dissimilar materials with several straight cracks subjected to anti-plane traction. Two kinds of property distributions for FGM coating, namely, $G(y) = G_0 e^{\beta y}$ and $G(y) = G_0(1 + \beta y)$ are studied. As the first example, we restrict our attention to the single crack located at interface with length $2c_1$ as shown in Fig. 2. The calculated SIFs at crack tips are normalized by $k_0 = \tau_0 \sqrt{c_1}$ where c_1 is the half length of crack and τ_0 is the constant traction distribution acts along the crack surface. The resulting values of the mode III normalized stress intensity factors with different gradient parameter for the ten different cases of relative crack length are listed in

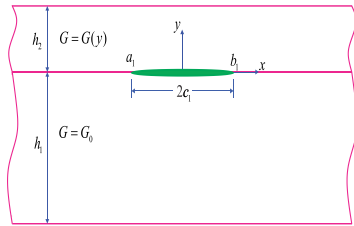


Fig. 2 Geometry of the one straight interface crack with length $2c_1$

Table 1 Comparisons of the normalized stress intensity factors for a crack in a medium with exponential material properties

c_1/h_2	$h_1/c_1=1.0$		$k_{III}/\tau_0\sqrt{c_1}$
	$\beta c_1=2\ln 0.5$	$\beta c_1=2\ln 1.0$	
Ding and Li (2008)			
0	1.2552	1.0930	0.9881
1	1.2877	1.1527	1.0405
2	1.3852	1.2739	1.1762
3	1.4954	1.4023	1.3155
4	1.5966	1.5199	1.4421
5	1.6869	1.6193	1.5543
6	1.7683	1.7080	1.6501
7	1.8387	1.7876	1.7387
8	1.9001	1.8563	1.8111
9	1.9561	1.9178	1.8780
10	2.0490	1.9805	1.9489
Present study			
0	1.2543	1.0911	0.9904
1	1.2845	1.1492	1.0406
2	1.3834	1.2738	1.1751
3	1.4919	1.3973	1.3087
4	1.5971	1.5125	1.4317
5	1.6970	1.6197	1.5450
6	1.7917	1.7200	1.6504
7	1.8817	1.8146	1.7490
8	1.9677	1.9042	1.8421
9	2.0499	1.9896	1.9304
10	2.1011	2.0713	2.0145

Tables 2 and 3 for exponential and liner properties, respectively. As it is seen from these two Tables, by increasing the value of relative crack length, the SIFs increase and also by increasing dimensionless non-homogeneity parameter, the SIFs decrease. The trend of normalized SIFs variation shows that when the material properties vary in the linear form, the values of normalized SIFs are higher than the case where the material properties vary in an exponential form. This may be due to the stiffness of material in an identical position of y coordinate; the case of linear form is less than against exponential form. Due to the symmetry, the stress intensity factors at the right and left crack tip are the same.

Figs. 3 and 4 show the effect of h_2/c_1 on the SIFs, for property distribution $G(y) = G_0 e^{\beta y}$ with $h_1/c_1=100$ and

Table 2 Stress intensity factors for property distribution $G(y) = G_0 e^{\beta y}$

c_1/h_1	$h_2/c_1=0.1$					$k_{III}/\tau_0\sqrt{c_1}$				
	$\beta h_2=-1$	$\beta h_2=-0.5$	$\beta h_2=0$	$\beta h_2=0.5$	$\beta h_2=1$	$\beta h_2=1.5$	$\beta h_2=2$	$\beta h_2=2.5$	$\beta h_2=3$	
1.0	2.5021	2.2827	2.0713	1.8717	1.6871	1.5206	1.3741	1.2487	1.1443	
0.9	2.3923	2.1852	1.9857	1.7972	1.6230	1.4658	1.3276	1.2092	1.1107	
0.8	2.2775	2.0833	1.8964	1.7198	1.5567	1.4096	1.2803	1.1696	1.0775	
0.7	2.1573	1.9767	1.8027	1.6386	1.4871	1.3505	1.2305	1.1279	1.0426	
0.6	2.0293	1.8636	1.7041	1.5537	1.4148	1.2898	1.1799	1.0861	1.0081	
0.5	1.8923	1.7431	1.5994	1.4640	1.3390	1.2264	1.1276	1.0433	0.9733	
0.4	1.7446	1.6135	1.4874	1.3685	1.2588	1.1602	1.0737	0.9999	0.9388	
0.3	1.5833	1.4726	1.3661	1.2659	1.1736	1.0906	1.0180	0.9561	0.9048	
0.2	1.4030	1.3165	1.2334	1.1553	1.0833	1.0188	0.9622	0.9141	0.8742	
0.1	1.1983	1.1437	1.0912	1.0416	0.9957	0.9542	0.9175	0.8860	0.8595	

Table 3 Stress intensity factors for property distribution $G(y) = G_0(1 + \beta y)$

c_1/h_1	$h_2/c_1=0.1$					$k_{III}/\tau_0\sqrt{c_1}$				
	$\beta h_2=-1$	$\beta h_2=-0.5$	$\beta h_2=0$	$\beta h_2=0.5$	$\beta h_2=1$	$\beta h_2=1.5$	$\beta h_2=2$	$\beta h_2=2.5$	$\beta h_2=3$	
1.0	2.7612	2.3270	2.0713	1.8977	1.7712	1.6744	1.5955	1.5315	1.4777	
0.9	2.6384	2.2271	1.9857	1.8219	1.7024	1.6108	1.5374	1.4755	1.4256	
0.8	2.5077	2.1225	1.8964	1.7431	1.6309	1.5446	1.4760	1.4199	1.3727	
0.7	2.3692	2.0127	1.8027	1.6605	1.5559	1.4762	1.4121	1.3597	1.3161	
0.6	2.2231	1.8967	1.7041	1.5734	1.4779	1.4040	1.3457	1.2975	1.2574	
0.5	2.0669	1.7731	1.5994	1.4817	1.3956	1.3291	1.2759	1.2325	1.1961	
0.4	1.8975	1.6399	1.4874	1.3839	1.3079	1.2497	1.2030	1.1646	1.1324	
0.3	1.7107	1.4945	1.3661	1.2788	1.2147	1.1651	1.1254	1.0932	1.0660	
0.2	1.4994	1.3329	1.2334	1.1651	1.1146	1.0756	1.0443	1.0185	0.9969	
0.1	1.2528	1.1529	1.0912	1.0473	1.0141	0.9880	0.9667	0.9489	0.9339	

Table 4 Stress intensity factors for property distribution $G(y) = G_0 e^{\beta y}$

βc_1	$k_{III}/\tau_0\sqrt{c_1}$						
	$h_2/h_1=0.1$	$h_2/h_1=0.2$	$h_2/h_1=0.3$	$h_2/h_1=0.4$	$h_2/h_1=0.5$	$h_2/h_1=0.75$	$h_2/h_1=1.0$
0.0	2.0713	1.6197	1.4367	1.3365	1.2738	1.1892	1.1492
0.1	2.0672	1.6142	1.4303	1.3295	1.2662	1.1808	1.1403
0.25	2.0610	1.6060	1.4208	1.3190	1.2551	1.1684	1.1272
0.5	2.0508	1.5924	1.4051	1.3018	1.2367	1.1483	1.1062
0.75	2.0406	1.5789	1.3895	1.2849	1.2188	1.1290	1.0863
1.0	2.0304	1.5655	1.3742	1.2682	1.2013	1.1104	1.0674
1.25	2.0202	1.5522	1.3590	1.2519	1.1842	1.0926	1.0498
1.5	2.0101	1.5390	1.3441	1.2359	1.1676	1.0756	1.0333
2.0	1.9899	1.5129	1.3147	1.2048	1.1358	1.0443	1.0039
2.5	1.9698	1.4873	1.2863	1.1752	1.1060	1.0165	0.9792
3.0	1.9499	1.4621	1.2588	1.1470	1.0783	0.9922	0.9588
5.0	1.8717	1.3660	1.1584	1.0500	0.9887	0.9254	0.9087

$h_1/c_1=1$, respectively. It is can be seen that SIFs decrease with increasing of dimensionless parameters βc_1 and h_2/c_1 .

Tables 4 and 5 show the effects of the non-homogeneity parameters and the FGM coating thickness on the stress intensity factors for both cases of material properties. It is can be seen that SIFs decrease with increasing βc_1 and h_2/h_1

Table 5 Stress intensity factors for property distribution $G(y) = G_0(1 + \beta y)$

βc_1	$k_{III} / \tau_0 \sqrt{c_1}$						
	$h_2/h_1=0.1$	$h_2/h_1=0.2$	$h_2/h_1=0.3$	$h_2/h_1=0.4$	$h_2/h_1=0.5$	$h_2/h_1=0.75$	$h_2/h_1=1.0$
0.0	2.0713	1.6197	1.4367	1.3365	1.2738	1.1892	1.1492
0.1	2.0673	1.6142	1.4304	1.3296	1.2664	1.1810	1.1405
0.25	2.0612	1.6062	1.4212	1.3196	1.2558	1.1695	1.1286
0.5	2.0512	1.5932	1.4065	1.3038	1.2393	1.1521	1.1110
0.75	2.0414	1.5808	1.3926	1.2891	1.2242	1.1367	1.0958
1.0	2.0317	1.5687	1.3794	1.2754	1.2102	1.1229	1.0824
1.25	2.0222	1.5570	1.3669	1.2626	1.1974	1.1105	1.0706
1.5	2.0129	1.5459	1.3550	1.2505	1.1855	1.0993	1.0601
2.0	1.9948	1.5245	1.3327	1.2284	1.1640	1.0796	1.0420
2.5	1.9771	1.5045	1.3125	1.2087	1.1450	1.0629	1.0269
3.0	1.9604	1.4857	1.2938	1.1909	1.1283	1.0485	1.0142
5.0	1.8977	1.4207	1.2325	1.1347	1.0769	1.0063	0.9779

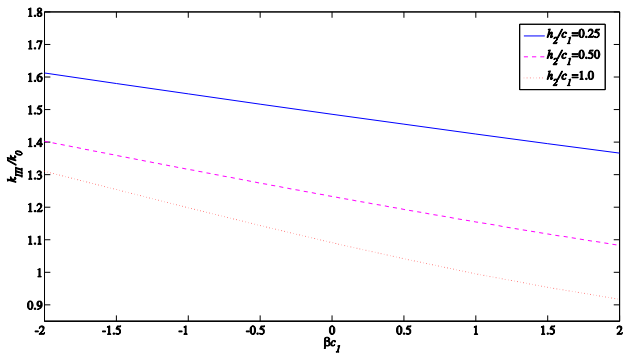


Fig. 3 The effect of h_2/c_1 on the SIFs with $h_1/c_1=100$

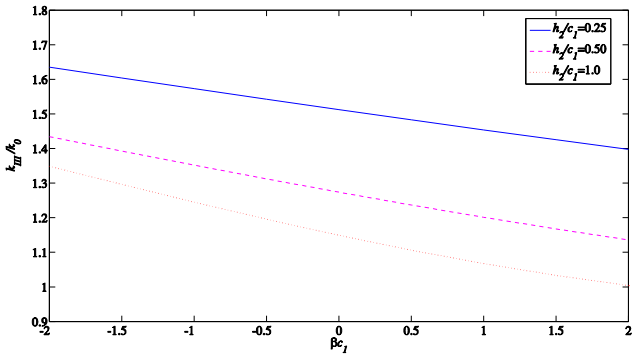


Fig. 4 The effect of h_2/c_1 on the SIFs with $h_1/c_1=1$

for both cases. In the next example, two unequal-length straight cracks a_1b_1 and a_2b_2 with lengths $2c_1$ and $2c_2$ respectively, as shown in Fig. 5. The distance between centers of two adjacent cracks is $2d$. The calculated SIFs at crack tips are normalized by $k_0 = \tau_0 \sqrt{c_1}$ where c_1 is the half length of crack a_1b_1 . The variation of dimensionless stress intensity factors for the different values of the non-homogeneity parameter, for two distances between center of cracks and for both cases of material properties are given in Tables 6-9 for both cases of material properties.

In comparison with the previous example, we observe that interaction between two cracks increases the stress

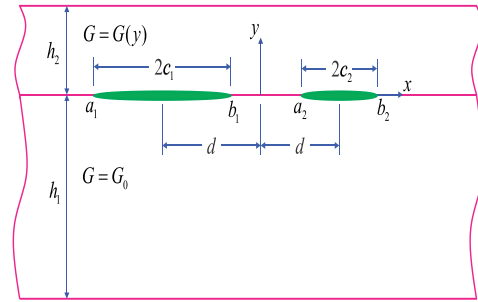


Fig. 5 Geometry of the two interface cracks

Table 6 Stress intensity factors for two interface cracks with property distribution $G(y) = G_0 e^{\beta y}$

βc_1	$c_2/c_1=0.75$ $h_2/h_1=0.1$ $(c_1+c_2)/d=0.75$			
	$k_{III}(a_1) / k_0$	$k_{III}(b_1) / k_0$	$k_{III}(a_2) / k_0$	$k_{III}(b_2) / k_0$
0.0	2.0765	2.1051	1.4276	1.3959
0.1	2.0724	2.1012	1.4252	1.3933
0.25	2.0663	2.0952	1.4215	1.3894
0.5	2.0561	2.0853	1.4153	1.3829
0.75	2.0459	2.0755	1.4092	1.3764
1.0	2.0358	2.0656	1.4031	1.3700
1.25	2.0257	2.0559	1.3970	1.3636
1.5	2.0156	2.0461	1.3910	1.3572
2.0	1.9956	2.0267	1.3789	1.3445
2.5	1.9757	2.0075	1.3670	1.3318
3.0	1.9559	1.9884	1.3552	1.3193
5.0	1.8783	1.9136	1.3091	1.2701

Table 7 Stress intensity factors for two interface cracks with property distribution $G(y) = G_0(1 + \beta y)$

βc_1	$c_2/c_1=0.75$ $h_2/h_1=0.1$ $(c_1+c_2)/d=0.75$			
	$k_{III}(a_1) / k_0$	$k_{III}(b_1) / k_0$	$k_{III}(a_2) / k_0$	$k_{III}(b_2) / k_0$
0.0	2.0765	2.1051	1.4276	1.3959
0.1	2.0725	2.1012	1.4252	1.3933
0.25	2.0664	2.0953	1.4215	1.3894
0.5	2.0565	2.0857	1.4155	1.3831
0.75	2.0467	2.0762	1.4097	1.3769
1.0	2.0370	2.0668	1.4039	1.3708
1.25	2.0276	2.0557	1.3982	1.3648
1.5	2.0184	2.0488	1.3927	1.3590
2.0	2.0004	2.0313	1.3818	1.3475
2.5	1.9830	2.0145	1.3714	1.3365
3.0	1.9663	1.9984	1.3614	1.3259
5.0	1.9042	1.9384	1.3264	1.2868

intensity factors of crack a_1b_1 . The SIFs at tip b_1 is larger than the other tips, stemming from the mutual effects of crack length and interaction with tip a_2 of crack a_2b_2 . According to Tables 6-9, it is also clear that the SIFs values go down with the increasing values of non-homogeneity parameter and the SIFs overall amount decrease with the increasing amount of crack distances.

Table 8 Stress intensity factors for two interface cracks with property distribution $G(y) = G_0 e^{\beta y}$

βc_1	$c_2/c_1=0.75$		$h_2/h_1=0.1$	$(c_1+c_2)/d=0.75$	
	$k_{III}(a_1)/k_0$	$k_{III}(b_1)/k_0$	$k_{III}(a_2)/k_0$	$k_{III}(b_2)/k_0$	
0.0	2.0982	2.3517	1.6987	1.4280	
0.1	2.0942	2.3483	1.6968	1.4255	
0.25	2.0882	2.3433	1.6939	1.4218	
0.5	2.0782	2.3348	1.6892	1.4156	
0.75	2.0682	2.3264	1.6845	1.4094	
1.0	2.0582	2.3181	1.6798	1.4032	
1.25	2.0483	2.3097	1.6752	1.3970	
1.5	2.0384	2.3015	1.6706	1.3909	
2.0	2.0188	2.2850	1.6614	1.3787	
2.5	1.9993	2.2686	1.6522	1.3666	
3.0	1.9799	2.2524	1.6432	1.3545	
5.0	1.9039	2.1890	1.6078	1.3075	

Table 9 Stress intensity factors for two interface cracks with property distribution $G(y) = G_0(1 + \beta y)$

βc_1	$c_2/c_1=0.75$		$h_2/h_1=0.1$	$(c_1+c_2)/d=0.75$	
	$k_{III}(a_1)/k_0$	$k_{III}(b_1)/k_0$	$k_{III}(a_2)/k_0$	$k_{III}(b_2)/k_0$	
0.0	2.0982	2.3517	1.6987	1.4280	
0.1	2.0942	2.3484	1.6968	1.4256	
0.25	2.0883	2.3434	1.6940	1.4219	
0.5	2.0784	2.3351	1.6894	1.4158	
0.75	2.0689	2.3270	1.6848	1.4098	
1.0	2.0596	2.3192	1.6805	1.4040	
1.25	2.0502	2.3112	1.6760	1.3982	
1.5	2.0412	2.3037	1.6718	1.3926	
2.0	2.0235	2.2888	1.6634	1.3817	
2.5	2.0066	2.2745	1.6554	1.3711	
3.0	1.9900	2.2605	1.6475	1.3608	
5.0	1.9292	2.2090	1.6187	1.3233	

5. Conclusions

In this paper, the fracture behavior of the several interface cracks located between two dissimilar materials by using of distributed dislocation technique has been studied. Two cases of material property models for shear modulus of FGM coating are considered. The problem is reduced to a set of singular integral equations with a Cauchy-type singular kernel by means of complex Fourier transform. Solving these integral equations with numerical method carried out and the stress intensity factors at the crack tips have been calculated. The effects of non-homogeneity parameter, relative crack length and thickness of FGM coating for two cases of material property on the SIF are discussed. It is found that, the magnitude of the SIF decreases with an increase of material gradient, coating thickness. The stress intensity factors increase with increasing of relative crack length. For the material properties vary along the thickness of the FGM layer linear form, the SIF is higher than the exponential form. The SIFs

in inner tips of the cracks are found to be greater than those in outer tips.

References

- Asadi, E. Fariborz, S.J. and Fotuhi, A.R. (2012), "Anti-plane analysis of orthotropic strips with defects and imperfect FGM coating", *Euro. J. Mech. A/Solids*, **34**, 12-20.
- Chiang, C.R. (1989), "Mode III interface crack propagation", *Eng. Fract. Mech.*, **32**, 545-550.
- Champion, C.R. and Atkinson, C.A. (1990), "Mode III crack at the interface between two nonlinear materials", *Proc. R. Soc. Series A, Math. Phys. Eng. Sci.*, **429**, 247-257.
- Chan, Y.S., Paulino, G.H. and Fannjiang, A.C. (2001), "The crack problem for nonhomogeneous materials under anti plane shear loading-a displacement based formulation", *Int. J. Solid. Struct.*, **38**, 2989-3005.
- Chen, Y.J. and Chue, C.H. (2009), "Mode III crack problems of two bonded functionally graded strips with internal cracks", *Int. J. Solids. Struct.*, **46**, 331-343.
- Chue, C.H. and Yeh, C.N. (2010), "Mode III fracture problem of two arbitrarily oriented cracks located within two bonded functionally graded material strips", *Meccanica*, **46**, 447-469.
- Cheng, Z., Gao, D. and Zhong, Z. (2012), "Interface crack of two dissimilar bonded functionally graded strips with arbitrary distributed properties under plane deformations", *Int. J. Mech. Sci.*, **54**, 287-293.
- Delale, F. and Erdogan, F. (1988), "Interface crack in a nonhomogeneous elastic medium", *Int. J. Eng. Sci.*, **26**, 559-568.
- Dag, S., Yildirim, B. and Erdogan, F. (2004), "Interface crack problems in graded orthotropic media, analytical and computational approaches", *Int. J. Fract.*, **130**, 471-496.
- Ding, S.H. and Li, X. (2008), "Anti-plane problem of periodic interface cracks in a functionally graded coating-substrate structure", *Int. J. Fract.*, **153**, 53-62.
- Erdogan, F., Gupta, G.D., and Cook, T.S. (1973), "Numerical solution of integral equations", Ed. Sih GC, *Methods of Analysis and Solution of Crack Problems*, Leyden, Holland, Noordhoff.
- Erdogan, F. (1985), "The crack problem for bonded nonhomogeneous materials under anti plane shear loading", *J. Appl. Mech.*, **52**, 823-828.
- Erdogan, F., Kaya, A.C. and Joseph, P.F. (1991), "The mode III crack problem in bonded materials with a nonhomogeneous interfacial zone", *J. Appl. Mech.*, **58**, 419-427.
- Erdogan, F. and Wu, B. (1993), "Interface crack problems in layered orthotropic materials", *J. Mech. Phys. Solid.*, **41**, 889-917.
- Farahpour, P., Babaghasabha, V. and Khadem, M. (2015), "Stress intensity factor calculation for semi-elliptical cracks on functionally graded material coated cylinders", *Struct. Eng. Mech.*, **55**, 1087-1097.
- Hills, D.A., Kelly, P.A., Dai, D.N. and Korsunsky, A.M. (1996), *Solution of Crack Problems: The Distributed Dislocation Technique*, Kluwer Academic Publishers.
- Jain, N., Rousseau, C.E. and Shukla, A. (2004), "Crack-tip stress fields in functionally graded materials with linearly varying properties", *Theor. Appl. Fract. Mech.*, **42**, 155-170.
- Jin, Z.H. and Batra, R.C. (1995), "Interface cracking between functionally graded coatings and a substrate under anti plane shear", *Int. J. Eng. Sci.*, **34**, 1705-1716.
- Kargarnovin, M.H., Nasirai, C. and Torshizian, M.R. (2011), "Anti-plane stress intensity, energy release and energy density at crack tips in a functionally graded strip with linearly varying properties", *Theor. Appl. Fract. Mech.*, **56**, 42-48.

- Lu, N.C., Cheng, J. and Cheng, Y.H. (2001), "Mode III interface crack propagation in two joined media with weak dissimilarity and strong orthotropy", *Theor. Appl. Fract. Mech.*, **36**, 219-231.
- Zhanqi, C. and Zheng, Z. (2006), "Fracture analysis of a functionally graded strip under plane deformation", *Acta. Mech. Solida. Sin.*, **19**, 114-121.
- Lu, N.C., Yang, D.N., Cheng, Y.H. and Cheng, J. (2007), "Asymmetrical dynamic propagation problems on mode III interface crack", *Appl. Math. Mech.*, **28**, 501-510.
- Li, Y.D., Tan, W. and Lee, K.Y. (2008), "Stress intensity factor of an anti-plane crack parallel to the weak/micro- discontinues interface in a bi-FGM composite", *Acta Mech. Solida. Sin.*, **21**, 34-43.
- Ming-Che, L. and Erdogan, F. (1983), "Stress intensity factors in two bonded elastic layers containing cracks perpendicular to and on the interface-I. Analysis", *Eng. Fract. Mec.*, **18**, 491-506.
- Ming-Che, L. and Erdogan, F. (1983), "Stress intensity factors in two bonded elastic layers containing cracks perpendicular to and on the interface-II. Solution and results", *Eng. Fract. Mech.*, **18**, 507-528.
- Monfared, M.M. and Ayatollahi, M. (2015), "Cracking in orthotropic half-plane with a functionally graded coating under anti-plane loading", *Acta. Mech. Solida Sin.*, **28**, 210-220.
- Monfared, M.M. and Bagheri, R. (2016), "Multiple interacting arbitrary shaped cracks in an FGM plane", *Theor. Appl. Fract. Mech.*, **86**, 161-170.
- Nakamura, T. (1991), "Three-dimensional stress fields of elastic interface cracks", *J. Appl. Mech.*, **58**, 939-946.
- Ren, J.H., Li, Y.S. and Wang, W. (2014), "A penny-shaped interfacial crack between piezoelectric layer and elastic half-space", *Struct Eng. Mech.*, **52**, 1-17.
- Torshizian, M.R. (2015), "Mode III stress intensity factor in two-dimensional functionally graded material with lengthwise linearly varying properties", *Arch. Appl. Mech.*, **85**, 2009-2021.
- Yang, W.Y., Zhang, S.Q., Li, J.L. and Ma, Y.L. (2009), "Interface crack problems for mode II of double dissimilar orthotropic composite materials", *Appl. Math. Mech.*, **30**, 585-594.